

Structural Characterization and Luminescent Properties of Poly(*p*-phenylene vinylene) and Poly(ethylene glycol) Blends

Horng-Long Cheng and King-Fu Lin*

Institute of Materials Science and Engineering, National Taiwan University, Taipei 10607, Taiwan, Republic of China

Abstract: The luminescent properties of poly(*p*-phenylenevinylene) (PPV) blending with poly(ethylene glycol) (PEG) were investigated in terms of their structural formation during sample preparation. The blended systems were prepared from an aqueous solution of water-soluble poly(xylylene tetrahydrothiophenium chloride) (PPV precursor) mixed with PEG, followed by heat treatment to remove the tetrahydrothiophene groups from the PPV precursor. Structural analysis showed that PEG could react with PPV precursor to form C-O-C linkage and carbonyl groups in PPV chains, interrupting their conjugated length as suggested by their Infrared, Raman and UV/vis spectroscopies. Wide angle X-ray scattering (WAXS) of blended systems also showed that PPV in blends had less packing. As to luminescent properties, the UV/vis and photoluminescent (PL) spectra show that the energy gap needed to produce the excitons increased along with the increase of PL intensity when PPV was blended with PEG. Similar results were also found for the EL properties of ITO/polyblends/Al devices. The EL light emission from blends was blue-shifted (compared to PPV) with a rather low threshold electric field strength. The EL performance of polyblends was better than that of pure PPV. Among them, the PPV-50PEG showed the highest EL intensity. The improved EL efficiency was attributed to the dilution effect, interrupted conjugated length, and lower packing of PPV chains.

Keywords: Poly(*p*-phenylene vinylene), Poly(ethylene glycol), Polyblends, Structure, Luminescent properties.

Introduction

Conjugated polymers having electroluminescent (EL) properties were first discovered by the Cambridge research group [1] in 1990 and demonstrated by using poly(*p*-phenylenevinylene) (PPV) as an active emissive layer in polymeric light-emitting diodes (polymeric-LEDs). Because of easy processing, polymeric-LEDs have the potential to be used in large-area display applications [1,2]. In recent years, many efforts have been made to improve their performance with respect to tuning the color of emitted light and increasing their luminescent quantum yield, brightness, stability, and processibility. Other endeavors have been aimed at developing of efficient ways of synthesizing the conjugated polymers [3-6].

One of the approaches to improve the performance of polymeric-LEDs is to blend conjugated

polymers with other polymers [7-18]. A number of conjugated/ nonconjugated polyblend systems have been studied with the aim of improving the atmospheric stability, processibility, and electroactivity [7-9]. It has been shown that their dilution of the conjugated polymer by other polymers in blends leads to an increase of the lifetime of luminescence [10,11]. In our previous study [12], we prepared the polymeric-LEDs by blending PPV with poly(*N*-vinylpyrrolidone) (PVP), a water-soluble nonconjugated polymer, and found that the optimal content of PVP in blends to provide the best EL performance was 15~20 wt%. Similar to our studies, Chang and Whang [13] prepared a series of PPV-poly(vinyl alcohol) (PVA) based polymers from the aqueous solutions of PPV precursor and PVA mixtures. Their PPV-PVA based LEDs emitted light from the green-yellow to the blue region by increas-

*To whom all correspondence should be addressed.
Tel: 886-2-2392-8290; Fax: 886-2-2363-4562
E-mail: kflin@ccms.ntu.edu.tw

J. Polym. Res. is covered in ISI (CD, D, MS, Q, RC, S), CA, EI, and Polymer Contents.

Table I. The compositions and energy gaps of PPV/PEG blends.

Sample denotation	Composition				Energy gap ^(a) (eV)
	PPV precursor		PEG		
	wt%	Molar ratio%	wt%	Molar ratio%	
PPV	100	100	0	0	2.37
PPV-20PEG	80	63.3	20	36.7	2.39
PPV-50PEG	50	30.1	50	69.9	2.40
PPV-80PEG	20	9.7	80	90.3	2.41
PEG	0	0	100	100	—

(a) Energy gap was determined by the onset of UV/vis absorption spectra using Eq.(2).

ing the content of PVA. This result was attributed to the fact that PPV precursor reacted with PVA to form C-O-C linkages and interrupted the PPV conjugated length.

In this study, we blended PPV with poly(ethylene glycol) (PEG), a water-soluble non-conjugated polymer. The blends have been used as an active polymer medium in newly developed light-emitting electrochemical cells, because PEG could effectively form the complexes with ions [19-21]. In this study, the structural formation during preparation of PPV/PEG blends was investigated first and the results were employed to interpret their photoluminescent properties and EL performance utilizing aluminum as an electron-injection electrode and indium-tin oxide (ITO) as a hole-injection electrode.

Experimental

1. Materials and sample preparation

The PPV precursor, poly(xylylene tetrahydrothiophenium chloride) (PXT) (polyelectrolyte) was prepared by following the ref. [3,4] with some modifications. The *p*-xylene-bis(tetrahydrothiophenium chloride) monomer (0.4 N) was dissolved in aqueous solution (20 mL) and then mixed with 80 mL pentane (pre-cooled to 0 °C). An equimolar quantity of sodium hydroxide (0.4 N, 20 mL) (pre-cooled to 0 °C) was afterwards added to the solution and reacted at 0 °C for 1 hour under nitrogen. The reaction was quenched by neutralization with 0.1 N HCl until the solution was slightly acidic, yielding a highly viscous solution. After the pentane was removed, the prepared PPV precursor solution was dialyzed in a Spectra/Por regenerated cellulose membrane tube with a molecular weight cut-off of 3,500 against deionized water for at least one week. The water surrounding the dialysis tube was refreshed frequently. At this stage, its PPV content measured from thermal gravimetric analysis (TGA) was ~0.25 wt%.

In order to overcome the inherent problems in

determining the molecular weight of PPV precursor, we replaced the ionic moieties with neutral thiophenolate groups by following the ref. [22]. The modified PXT compound had a M_w of 1.2×10^6 and dispersity of 3.2 relative to the polystyrene standards, measured by gel permeation chromatography (Testhigh Series III pump and Model 500 UV detector with THF as a mobile phase).

Poly(ethylene glycol) (PEG), purchased from the Jassen Co. and having a molecular weight of 4×10^4 , was dried under a vacuum at 50 °C for 12 hours and used without further purification.

Blended solutions of PPV precursor with PEG were prepared by adding various amounts of PEG to the precursor aqueous solutions and mixed until homogeneous. We designated the prepared solution containing 20 wt% PEG as PPV-20PEG, and so on as shown in Table I. Films were prepared by spin-coating the solution onto glass plates. Transformation of the PPV precursor into PPV was achieved by heating the films in a high vacuum oven ($< 10^{-5}$ torr) at 220 °C for 2 hours. The final thickness of the films on the glass plates prepared for PL measurements was controlled at 1000~1300 Å, measured by using a surface profilometer (Dektak Co., Model 3030).

2. Fabrication of LEDs

LEDs were fabricated by spin-coating the polymer solution onto indium-tin oxide (ITO)-deposited glass plates and heat treating them at 220 °C for 2 hours, followed by Al metal evaporation (thermal evaporator, JEOL Co. Model JEE-4C) to form the electron injection electrode. The polymer films and the coated Al electrode should be uniform, with thicknesses ranging from 1000~1300 and 1500~2000 Å, respectively, measured by using a surface profilometer (Dektak Co., Model 3030). Active areas of each device were 3 mm².

3. Characterization

Infrared spectra of polymer films (removed from the coated glass plates) were recorded on a

Jasco 300E model FTIR spectrometer. Their Raman spectra excited by a He-Ne laser (632.8 nm) were recorded on a Renishaw 127 model Raman spectrometer. Wide-angle X-ray spectroscopy (WAXS) of polymer films was performed on a Philips model PW1710 X-ray diffractometer using Cu-K α radiation and a graphite monochromator. Thermogravimetric analysis (TGA) of polymer films was performed using a Du pont 9900-954 TGA system under nitrogen at a heating rate of 10 °C/min from 30 to 550 °C. Their ultraviolet/visible (UV/vis) absorption spectra were recorded on a Jasco-555 model spectrometer. Photoluminescent (PL) spectra of the films on glass plates were measured by subjecting the films to ultraviolet light with a wavelength of 365 nm and the results were recorded on a Jasco FR-777 spectrofluorometer. The EL spectra of the ITO/polymer/Al sandwich devices at a drive voltage of 8 volts (V) were also recorded on the same spectrofluorometer. The current density-electric field strength (I-E) characteristic of the devices was measured by a Keithley 2400 model electrometer, where the concurrent EL intensities were recorded by using a photodiode detector. All characterizations were made at room temperature in a laboratory environment.

Results and Discussion

1. Structural analysis

1.1 Chemical structure

Figure 1 shows the IR spectra of the polymer films of PPV, PEG and PPV/PEG blends. In Figure 1(a), the PPV shows a strong absorption at 965 and 3024 cm $^{-1}$, contributed by the trans-vinylene C-H out-of-plane bending and trans-vinylene C-H stretching mode, respectively [23-25]. The bands near 555 and 837 cm $^{-1}$ are due to the phenylene out-of-plane ring bending and para-phenylene ring C-H out-of-plane bending, respectively. The absorption bands near 1515 and 1423 cm $^{-1}$ are related to the *p*-phenylene semi-ring stretching mode. These major absorption bands were also seen in PPV/PEG blends (shown in Figures 1(b)-1(d)); however, in blends, the absorption peaks at 965 and 3024 cm $^{-1}$ drastically decreased with the content of PEG. The absorption bands of PPV/PEG blends near 2850 and 2930 cm $^{-1}$ are due to the aliphatic C-H stretching mode and those at 1100 and 1060 cm $^{-1}$ are due to the C-O-C bending of PEG units. In addition, a new absorption band in the region 1650-1750 cm $^{-1}$ signals the presence of the carbonyl group (C=O) in blends. These results indicate that the blended materials after heat treatment may not be viewed as a pure physical mixture of PPV and PEG; instead, they

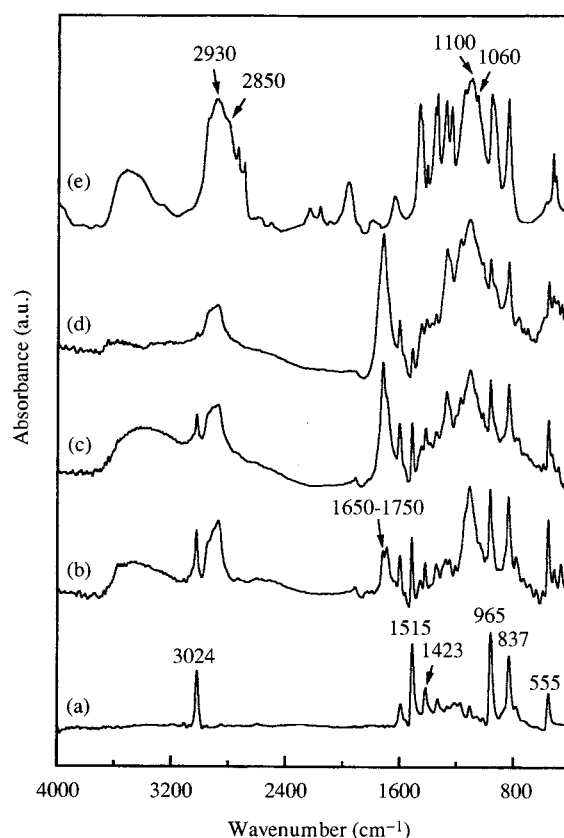


Figure 1. FT-IR spectra of (a) PPV, (b) PPV-20PEG, (c) PPV-50PEG, (d) PPV-80PEG and (e) PEG.

undergo some side reactions. To estimate the fraction of non-conjugated part of PPV in blends due to chemical reactions with PEG, we compared the absorptions of trans-vinylene CH stretching peak (3024 cm $^{-1}$) of the blended sample with PPV by choosing the *p*-phenylene semicircle stretching peak (1515 cm $^{-1}$) as a reference peak. The estimated fractions of non-conjugated part of PPV in blends were 0.18, 0.46, and 0.74 for PPV-20PEG, PPV-50PEG, and PPV-80PEG, respectively, if neat PPV was assumed to have perfect conjugated sequence. Apparently, the non-conjugated part of PPV increased with the content of PEG.

The mutual reactions of polymers in blends were further investigated by extraction experiments. The fully transformed PPV in PPV/PEG blends is insoluble in all common solvents [9] and only the PEG component is extractable. The converted films were extracted with chloroform because of its high volatility and good solvating power for PEG. The results of the extraction experiment are shown in Figure 2. In Figure 2(a), the insoluble part shows the major absorbances similar to the PPV (e.g. the absorption peaks at 965 and 3024 cm $^{-1}$). The C-O-C stretching mode (at 1060 and 1100 cm $^{-1}$) and the

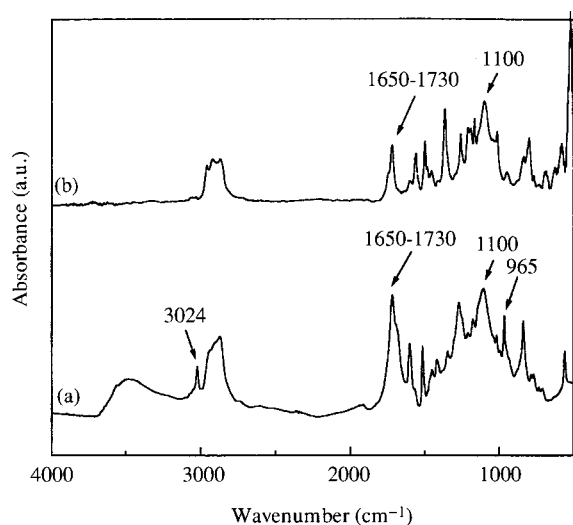


Figure 2. FT-IR spectra of (a) chloroform-insoluble portion and (b) chloroform-extractable portion of PPV-50PEG.

aliphatic C-H stretching mode (at 2850 and 2930 cm^{-1}) from PEG are also seen, in addition to an extra peak at 1650~1730 cm^{-1} assigned to the carbonyl group. In Figure 2(b), the extracted part only shows the absorbances from PEG and the carbonyl groups, the molecular weight of which is about 1000~1500 measured by GPC, much smaller than the initial M_w of PEG.

It should be noted that since the tetrahydrothiophene (THT) group in PPV precursor is a good leaving group [26,27], a wider range of polymers may be blended successfully with PPV [7-9]. A previous study of PPV/poly(acrylamide) (PAA) blends showed evidence of reaction of the PAA component with HCl yielded during the conversion reaction [7]. In another system, PPV/poly(vinyl methyl ether) (PVME) blends, their IR spectra also showed new bands at 1720 and 1690 cm^{-1} contributed by the carbonyl groups as a result of thermal degradation of PVME during the conversion reaction [8]. Chang and Whang [13] prepared PPV-PVA-based polymers through heat treatment of a mixture of PPV precursor with PVA and showed that PPV precursor could react with PVA to form the C-O-C linkage and interrupt the PPV conjugated length. Similarly, PEG was also involved in the conversion reactions of PPV precursor. Considering the above results, we could presume that the C-O-C groups of PEG could react with the PPV precursor during the elimination of THT groups of PPV precursor along with the scission of PEG chains and that they could form carbonyl groups. The chemical reactions are suggested as shown in Figure 3. Apparently, introducing PEG into PPV reduces the conjugated length of PPV chains.

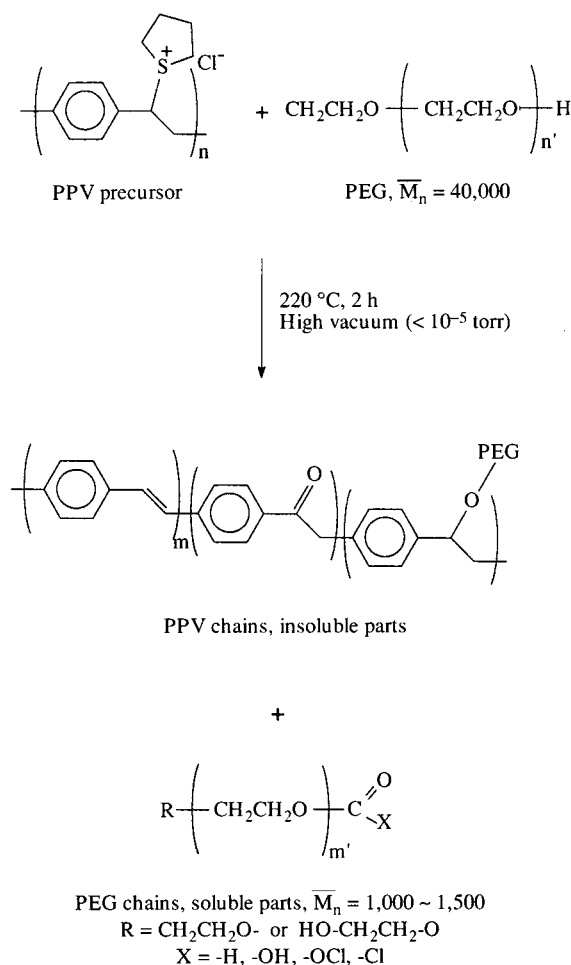


Figure 3. Schematic representation of possible chemical reactions between PPV precursor and PEG.

1.2 Structural analysis by Raman spectroscopy

Raman spectroscopy has been proven to be an effective method of probing the extent of delocalization in conjugated materials through the change in vibrational frequencies associated with changes in the strength of bond-alternation.

Figure 4 shows the Raman spectra of PPV and PPV/PEG blends excited by a wavelength of 632.8 nm. The Raman spectrum of PPV has been well studied [23-25,28]. The main bands which peaked at 1331 and 1629 cm^{-1} were the results of vinylenic C=C stretching; those peaked at 1550 and 1587 cm^{-1} were the results of phenylene C-C ring stretching; the peak at 1173 cm^{-1} was the results of phenylene C-H ring in-plane bending. The appearance of a very weak 967 cm^{-1} band caused by the vinylenic C-H out-of-plane bending was indicated as evidence of slight distortion of the vinylenic group from a planar trans form of PPV polymer chains [25]. According to their studies, PPV conjugated segments in a solid state have approximate C_{2h} symmetry. In Figure 4, the Raman spectra of all the

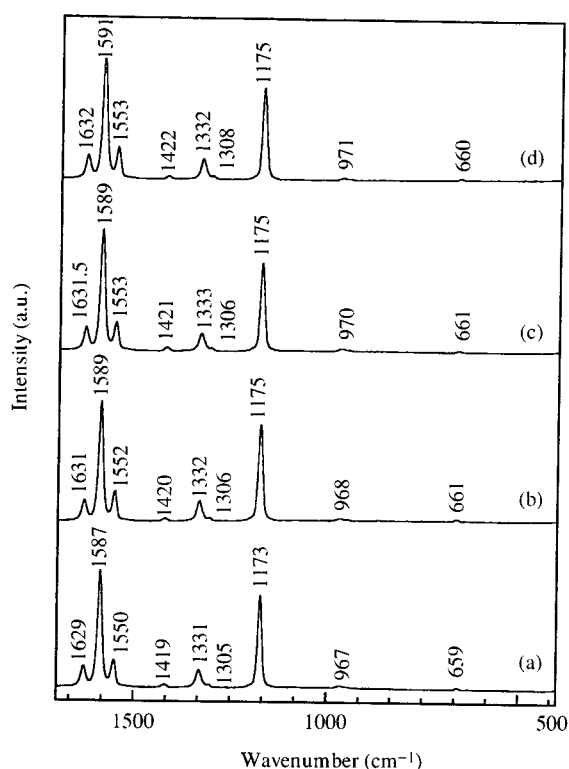


Figure 4. Raman spectra of (a) PPV, (b) PPV-20PEG, (c) PPV-50PEG and (d) PPV-80PEG.

samples were similar, except that the positions of these bands were shifted to higher frequencies by increasing the content of the PEG component in blends. According to Tian et al. [24], the PPV chains with shorter conjugated length have higher vibrational frequencies in Raman spectra. Moreover, the dilution of PPV by other polymers such as PVP without any chemical reaction would not cause any shifting of those bands [12]. As a result, it follows that the conjugated length of PPV chains in blends was reduced by reaction with PEG.

1.3 Structural analysis by WAXS

Figure 5 shows the WAXS patterns of PPV, PEG, and PPV/PEG blends. In Figure 5(a), the diffraction pattern of pure PPV is in agreement with that reported in the literature [29,30], that is, the corresponding unit cell is a rectangular P2gg two-dimensional space group projection of a monoclinic unit cell. The d -spacings of (110), (200), and (210) are 4.29 ($2\theta = 20.7^\circ$), 3.95 ($2\theta = 22.5^\circ$), and 3.19 Å ($2\theta = 28^\circ$), respectively. According to the assignment, the (110) and (200) reflections overlap. In Figure 5(e), the WAXS pattern of PEG with two pronounced peaks at $2\theta = 19^\circ$ and $2\theta = 23^\circ$ is typical for a highly crystallized PEG. The primary difference between the WAXS patterns of PPV/PEG

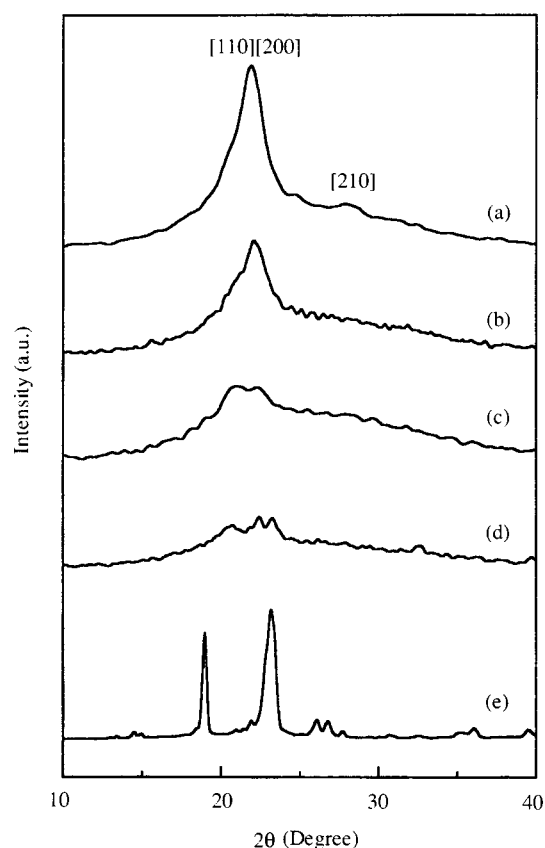


Figure 5. WAXS patterns of (a) PPV, (b) PPV-20PEG, (c) PPV-50PEG, (d) PPV-80PEG and (e) PEG.

blends and pure PPV is the reduction of intensity of the (110) and (200) reflections with increasing content of PEG. The WAXS pattern of PPV/PEG blends shown in Figure 5(b)~(d) is similar to the reported patterns of incompletely transformed PPV, which indicates that the imperfect PPV crystalline co-existed with the amorphous PPV precursor [31]. When the precursor was transformed more, the crystalline domains had better packing and their size increased. Briefly speaking, PEG in the blend could impede the packing of PPV chains; this phenomenon is referred to as the "dilution effect" [7,12].

2. Luminescent properties

2.1 Optical absorption

Figure 6 shows the UV/vis spectra of PPV and its blends with PEG. The energy gap, E , of the π - π^* interband onset transition to yield the exciton can be calculated by the following equation,

$$E = 1240 / \lambda \quad (1)$$

where λ is the onset of the UV/vis absorption wavelength. From Eq.(1), the calculated energy gap

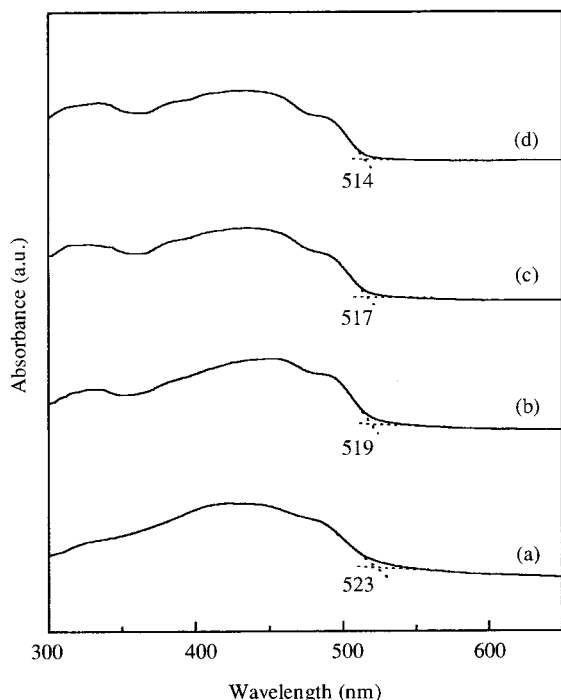


Figure 6. UV/vis spectra of (a) PPV, (b) PPV-20PEG, (c) PPV-50PEG and (d) PPV-80PEG.

of PPV and of PPV/PEG blends is listed in Table I. The onset of UV/vis absorption of PPV/PEG blends shifted to a higher energy (blue shift) as the PEG content was increased.

2.2 Photoluminescent spectra

Figure 7 shows the PL spectra of PPV and its blends with PEG excited by UV light at a wavelength of 365 nm. The major peaks in the PL spectrum of PPV chromophore at 520 and 550 nm have been referred to as the 0-0 and 0-1 vibronic emission [32]. However, by introducing PEG in blended systems, there was a slight blue shift in the PL spectra due to the shorter conjugated length of PPV chains. Because only PPV conjugated chains emit fluorescent light, to evaluate the effect of blending on the luminescent properties of PPV we calculated the relative intensities, RI , of 0-0 and 0-1 vibronic peaks per mole of PPV conjugated unit by the following equation [12]

$$RI = I_b / (x_p I_p) \quad (2)$$

where I_b and I_p are the peak intensity of blends and of pristine PPV, respectively, and x_p is the molar fraction of PPV in blends. The results were plotted in Figure 8, indicating that emission intensities of PPV were increased by blending with PEG and that the 0-0 vibronic peak was increased even more.

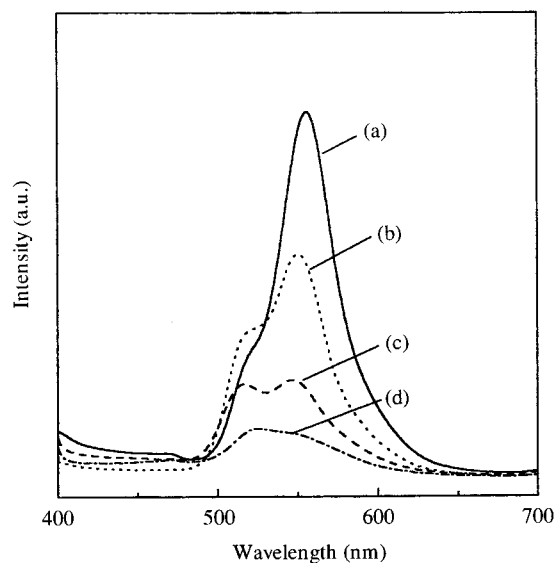


Figure 7. Photoluminescent spectra of (a) PPV, (b) PPV-20PEG, (c) PPV-50PEG, and (d) PPV-80PEG, measured at 298 K by UV excitation at 365 nm.

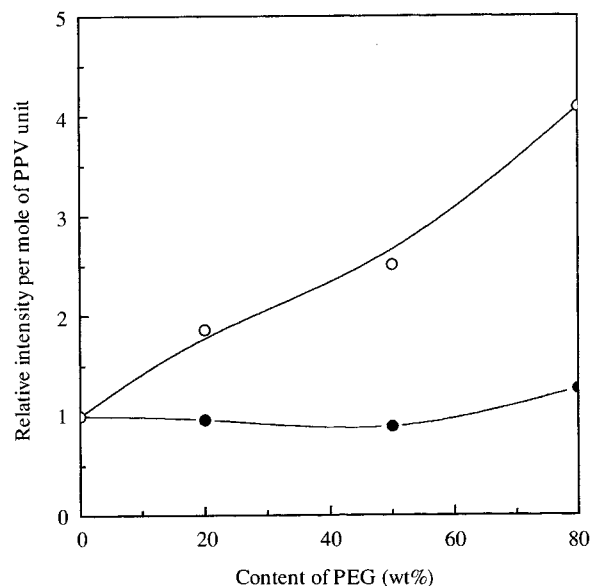


Figure 8. Relative intensities of (O) 0-0 (~520 nm) and (●) 0-1 (~550 nm) vibronic emissions per mole of PPV conjugated units as a function of PEG content in PPV/PEG blends.

2.3 Electroluminescent spectra

Figure 9 shows the EL spectra of ITO/polymer/Al LED devices incorporating PPV and its blends with PEG respectively, at a drive voltage of 8 V (or at an electric field strength of 6×10^7 V/m). ITO was used as a hole-injection electrode, whereas Al was used as an electron-injection electrode. The EL spectrum of PPV LEDs is basically the same as the PL spectrum except that the intensity of the 0-0

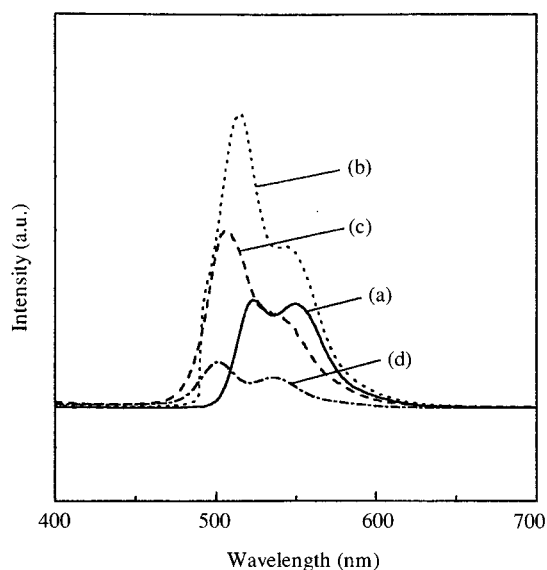


Figure 9. Electroluminescent spectra of ITO/Polymer/Al LEDs incorporating (a) PPV, (b) PPV-20PEG, (c) PPV-50PEG, and (d) PPV-80PEG.

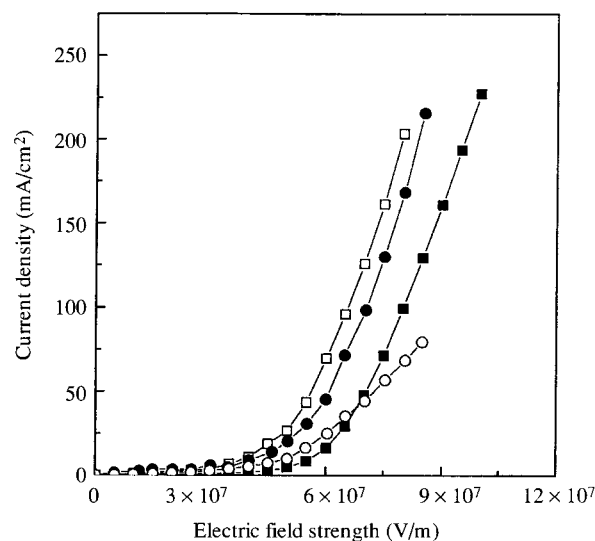


Figure 10. Current density-electric field strength characteristics of LEDs incorporating (■) PPV, (□) PPV-20PEG, (●) PPV-50PEG, and (○) PPV-80PEG.

vibronic peak is relatively higher. When PPV was blended with 20 wt% or more PEG, the EL spectrum was broader with a remarkable blue shift and had much higher intensity compared to the pristine PPV. PPV-20PEG and PPV-50PEG emitted yellow-green light with two emission peaks at 515 and 545 nm and at 505 and 538 nm, respectively. However, with a further increase of the PEG content, the emission intensity decreased. The 0-1 vibronic peak reduced its intensity at a much higher rate than the 0-0 vibronic peak. When the content of PEG was increased to 80 wt%, the vibronic peaks were further shifted to a smaller wavelength. The blue shift found in UV/vis, PL, and EL spectra is consistent with the observed shorter conjugation length of PPV by increasing the PEG content in blends.

2.4 Other LED characteristics

Figure 10 illustrates the current density-electric field strength (I - E) characteristics of LED devices incorporating PPV and its blends with PEG respectively. When the forward E strength exceeded the threshold E strength, a yellow-green light was emitted. It can be seen from the figure that the threshold E strength of PPV devices was decreased from 5×10^7 to 3×10^7 V/m by blending with 20 wt% PEG. Further increase of PEG content to 80 wt% increased the threshold E strength of devices to 4.5×10^7 V/m. Figure 11 illustrates the concurrent EL intensities emitted by devices as a function of the applied electric field strength. Since EL is emitted by the singlet excitons generated by means of the annihilation between the injected holes and electrons

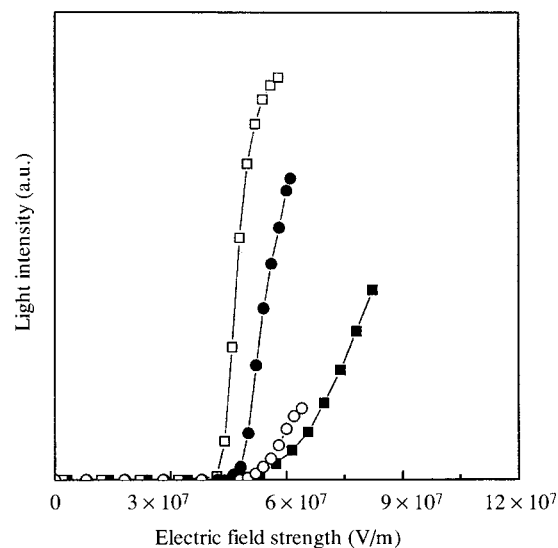


Figure 11. EL intensity-electric field strength curves of LEDs incorporating (■) PPV, (□) PPV-20PEG, (●) PPV-50PEG, and (○) PPV-80PEG.

from the electrodes, a higher current produces more excitons and hence gives off higher EL intensity. This phenomenon can be seen in Figure 12 illustrating the EL intensities per mole of PPV conjugated units as a function of the current density in the devices. The figure was plotted by rearrangement of the data from Figures 10 and 11 based on the uniform current density across the specimen. As seen in the Figure, the PPV phase in PPV/PEG blends emitted higher EL intensity than pure PPV based on the same current density. The highest EL intensity

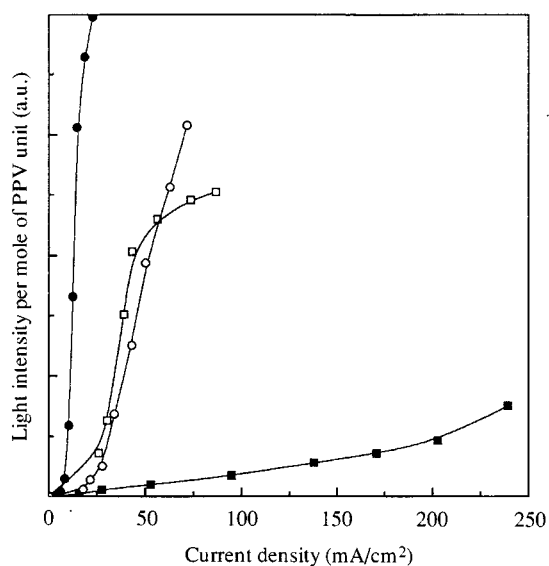


Figure 12. EL intensity per mole of PPV units as a function of current density in LEDs incorporating (■) PPV, (□) PPV-20PEG, (●) PPV-50PEG, and (○) PPV-80PEG.

found in PPV-50PEG was about 80 times greater than that of pure PPV under the same current density of $\sim 25 \text{ mA/cm}^2$.

The improvement of PL and EL efficiencies of PPV by blending may be explained by the following factors. First, the dilution effect that the generated excitons had little tendency to undergo the non-radiation decay through the interchain's quenching increases the luminescent efficiencies. A similar phenomenon was observed in PPV/PVP blends [12], poly(2-methoxy-5-(2-ethylhexyloxy-1,4-phenylenevinylene) (MEH-PPV)/poly(methyl metacrylate) (PMMA) blends [10], and poly(phenyl-*p*-phenylenevinylene)/polycarbonate blends [11]. Yan et al. [33] have also indicated that PL efficiency could be increased by separating the conjugated polymer chains. Second, introducing disorders or non-conjugated segments into PPV chains by PEG played an important role in enhancing the luminescence. Staring et al. [34] suggested that the presence of non-conjugated segments confines the excitons in the conjugated segments of the chain and prevents their non-radiative decay.

On the other hand, according to Papadimitrakopoulos et al. [35,36], the PL intensity of PPV exhibits a dramatic reduction with increasing the content of carbonyl groups. Their data suggested that carbonyl groups act as a quenching site and greatly reduce the PL intensity. Although PPV/PEG blends generated some carbonyl groups during sample preparation, we did not observe a similar reduction of PL and EL intensities.

Conclusion

A series of PPV/PEG polyblends as light emitting materials were prepared through the heat treatments of the mixtures of PPV precursors with PEG in aqueous solutions. Structural analysis showed that the PPV/PEG blends were not a pure physical blend, rather that the PEG not only diluted (or unpacked) the PPV crystallized chains but also disrupted (or shortened) their conjugated length. As a result, the energy gap of polyblends was increased with the content of PEG. Their PL and EL spectra also showed a detectable blue shift, with an emitting color changing from yellow-green (550 and 520 nm) to near green (530 and 500 nm) by increasing the content of PEG. The LED devices prepared from PEG/PPV polyblends had lower threshold electric field strength, about $3\sim 4 \times 10^7 \text{ V/m}$ lower than that from pure PPV, and had better luminescent efficiency as well. Among blends, the PPV-50PEG showed the highest EL efficiency, with light intensity per mole of PPV unit 80 times greater than that of pure PPV under the same current density of $\sim 25 \text{ mA/cm}^2$.

Acknowledgment

The authors would like to acknowledge the financial support of the National Science Council in Taiwan, Republic of China through Grant NSC 87-2216-E-002-01.

References

1. J. H. Burroughes, D. D. C. Bradley, A. R. Brown, R. N. Marks, K. Mackay, R. H. Friend, P. L. Burn and A. B. Holmes, *Nature*, **347**, 539 (1990).
2. D. Braun and A. J. Heeger, *Appl. Phys. Lett.*, **58**, 1982 (1991).
3. R. A. Wessling, *J. Polym. Sci., Polym. Symp.*, **72**, 55 (1985).
4. R. W. Lenz, C. C. Han, J. Stenger-Smith and F. E. Karasz, *J. Polym. Sci., Polym. Chem.*, **26**, 3241 (1988).
5. R. M. Gregorius, P. M. Lahti and F. E. Karasz, *Macromolecules*, **25**, 6664 (1992).
6. P. L. Burn, A. B. Holmes, A. Kraft, D. D. C. Bradley, A. R. Brown, R. H. Friend and R. W. Gymer, *Nature*, **356**, 47 (1992).
7. J. M. Machado, F. E. Karasz and R. W. Lenz, *Polymer*, **29**, 1412 (1988).
8. J. B. Schlenoff, J. M. Machado, P. J. Glatkowski and F. E. Karasz, *J. Polym. Sci., Polym. Phys. Ed.*, **26**, 2247 (1988).
9. J. M. Machado, J. B. Schlenoff and F. E. Karasz, *Macromolecules*, **22**, 1964 (1989).
10. L. Smilowitz, A. Hays, A. J. Heeger, G. Wang and J. E. Bowers, *J. Chem. Phys.*, **98**, 6504 (1993).
11. U. Lemmer, R. F. Mahrt, Y. Wada, A. Greiner, H.

- Bassler and E. O. Gobel, *Appl. Phys. Lett.*, **62**, 2827 (1993).
12. K. F. Lin, L. K. Chang and H. L. Cheng, *Polym. Prepr.*, **38**, 544 (1997).
 13. W. P. Chang and W. T. Whang, *Polymer*, **37**, 3493 (1996).
 14. G. Yu., H. Nishino, A. J. Heeger, T. A. Chen and R. D. Rieke, *Synth. Met.*, **72**, 249 (1995).
 15. I. N. Kang, D. H. Hwang, H. K. Shim, T. Zyung and J. J. Kim, *Macromolecules*, **29**, 165 (1996).
 16. F. Hide, C. Y. Yang and A. J. Heeger, *Synth. Met.*, **85**, 1335 (1997).
 17. J. Huang, H. Zhang, W. Tian, J. Hou, Y. Ma, J. Shen and S. Liu, *Synth. Met.*, **87**, 105 (1997).
 18. S. A. Chen, E. C. Chang, K. R. Chuang, C. I. Chao, J. H. Hsu, P. K. Wei and W. S. Fann, *Polym. Prepr.*, **39**, 105 (1998).
 19. Q. Pei, G. Yu, C. Zhang, Y. Yang and A. J. Heeger, *Science*, **269**, 1086 (1995). 20. Y. Yang and Q. Pei, *Appl. Phys. Lett.*, **68**, 2708 (1996).
 21. Q. Pei, Y. Yang, G. Yu, Y. Cao and A. J. Heeger, *Synth. Met.*, **85**, 1229 (1997).
 22. J. M. Machado, F. R. Denton III, J. B. Schlenoff, F. E. Karasz and P. M. Lahti, *J. Polym. Sci., Polym. Phys.*, **27**, 199 (1989).
 23. D. Rakovic, R. Kostic, L. A. Gribov and I. E. Davidova, *Phys. Rev. B*, **41**, 10745 (1990).
 24. B. Tian, G. Zerbi, R. Schenk and K. Mullen, *J. Chem. Phys.*, **95**, 3191 (1991).
 25. A. Sakamoto, Y. Furukawa and M. Tasumi, *J. Phys. Chem.*, **96**, 1490 (1992).
 26. P. L. Burn, D. D. C. Bradley, R. H. Friend, D. A. Halliday, A. B. Holmes, R. W. Jackson and A. Kraft, *J. Chem. Soc., Perkin. Trans.*, **1**, 3225 (1992).
 27. D. A. Halliday, P. L. Burn, R. H. Friend, D. D. C. Bradley and A. B. Holmes, *Synth. Met.*, **55-57**, 902 (1993).
 28. S. Lefrant, E. Perrin, J. P. Buisson, H. Eckhardt and C. C. Han, *Synth. Met.*, **29**, E91 (1989).
 29. T. Granier, E. L. Thomas, D. R. Gagnon, F. E. Karasz and R. W. Lenz, *J. Polym. Sci., Polym. Phys.*, **24**, 2793 (1986).
 30. D. Chen, M. J. Winokur, M. A. Masse and F. E. Karasz, *Polymer*, **33**, 3116 (1992).
 31. T. A. Ezquerro, E. Lopez-Cabarcos, F. J. Balta-Calleja, J. D. Stenger-Smith and R. W. Lenz, *Polymer*, **32**, 781 (1991).
 32. B. Hu and F. E. Karasz, *Chem. Phys.*, **227**, 263 (1998).
 33. M. Yan, L. J. Rothberg, F. Papadimitrakopoulos, M. E. Galvin and T. M. Miller, *Phys. Rev. Lett.*, **73**, 744 (1994).
 34. E. G. J. Staring, R. C. J. E. Demandt, D. Braun and G. L. J. Rikken, *Adv. Mater.*, **6**, 934 (1994).
 35. F. Papadimitrakopoulos, K. Konstadinidis, T. M. Miller, R. Opila, E. A. Chandross and M. E. Galvin, *Chem. Mater.*, **6**, 1563 (1994).
 36. F. Papadimitrakopoulos, M. Yan, L. J. Rothberg, H. Katz, E. A. Chandross and M. E. Galvin, *Mol. Cryst. Liq. Cryst.*, **256**, 663 (1994).